



# DALHOUSIE UNIVERSITY

Retrieved from DalSpace, the institutional repository of  
Dalhousie University

<https://dalspace.library.dal.ca/handle/10222/73087>

Version: Post-print

**Publisher's version:** Sadeghian, Pedram, Rahai, Ali R, and Ehsani, Mohammad R. (2009).  
Effect of Fiber Orientation on Nonlinear Behavior of CFRP Composites. *Journal of Reinforced Plastics and Composites*, 28 (18), 2261-2272. doi: 10.1177/0731684408092065

# Effect of Fiber Orientation on Nonlinear Behavior of CFRP Composites

Pedram Sadeghian <sup>a,\*</sup>, Ali R. Rahai <sup>b</sup>, and Mohammad R. Ehsani <sup>c</sup>

<sup>a</sup> Department of Civil and Architectural Engineering, Islamic Azad University of Qazvin, Nokhbegan Blvd., Daneshgah St., Qazvin, Iran

<sup>b</sup> Department of Civil and Environmental Engineering, Amirkabir University of Technology No. 424, Hafez St., Enghelab Av., Tehran, Iran

<sup>c</sup> Department of Civil Engineering and Engineering Mechanics, University of Arizona Bldg. No. 72, Room 206, Tucson, AZ 85721, USA

\* Corresponding author. Tel.: +98-912-200-2568; fax: +98-21-8879-6665

E-mail address: [Pedrad@yahoo.com](mailto:Pedrad@yahoo.com) & [Sadeghian@aut.ac.ir](mailto:Sadeghian@aut.ac.ir) (P. Sadeghian)

## Abstract

Fiber orientation is one of the important parameters that affect strength and ductility of FRP-confined concrete columns. A number of studies have been conducted on various fiber orientations and wrap thicknesses, but have not been carried out a comprehensive study on tensile properties of FRP with various fiber orientations and their effects on confined concrete. This paper presents the results of experimental studies about mechanical properties of CFRP composites. In this study, 24 coupons of CFRP composites were prepared and tested in axial tension under displacement control mode. Eight ply configurations were prepared with fibers oriented at  $0^\circ$ ,  $\pm 45^\circ$ , and  $90^\circ$  from the axial direction and with 1, 2, 3, and 4 plies. It was found that stress-strain behavior basically depended on fiber orientation. The behavior in on-axis orientation showed perfectly linear-elastic with brittle rupture, but in off-axis orientation showed

1  
2  
3  
4 fully nonlinear with high ductility. An analytical model proposed for the nonlinear  
5  
6 behavior of composites with off-axis orientation.  
7  
8

9  
10  
11 **Keywords:** CFRP, fiber orientation, nonlinear, ductility, confinement, strengthening,  
12  
13 concrete column.  
14  
15

## 16 17 18 19 **1. Introduction**

20  
21 In recent years, strengthening of reinforced concrete structures has become a  
22  
23 great challenge for civil engineering professionals. Fiber Reinforced Polymer (FRP)  
24  
25 composites are very suitable materials that offer unique advantages for repair and  
26  
27 retrofit of structures. These materials have high tensile strength, light weight, high  
28  
29 modulus and corrosion resistance. Their flexibility allows them to be wrapped around  
30  
31 various concrete elements with different geometries, especially column sections.  
32  
33

34  
35 Previous researches have indicated that wrapping with FRP jackets or straps  
36  
37 significantly increase the strength and ductility of poorly detailed columns. This  
38  
39 increase in strength emanates from the passive confinement pressure of the FRP jackets  
40  
41 [1]. Design of FRP-wrapped concrete has come a long way from the early applications  
42  
43 of steel-based models such as that of Mander et al. [2] to recognize that such models fail  
44  
45 to capture the true behavior of FRP-confined concrete [3]. This is mainly due to the  
46  
47 unique dilation characteristics of concrete when confined by linear-elastic and non-  
48  
49 yielding materials such as FRP [4]. The performance of unidirectional FRP laminates is  
50  
51 highly dependent on fiber orientation with respect to applied load direction [5]. So fiber  
52  
53 orientation is one of the important parameters that affect strength and ductility of FRP-  
54  
55 confined concrete columns [6].  
56  
57  
58  
59  
60

1  
2  
3  
4  
5  
6  
7  
8  
9  
10  
11  
12  
13  
14  
15  
16  
17  
18  
19  
20  
21  
22  
23  
24  
25  
26  
27  
28  
29  
30  
31  
32  
33  
34  
35  
36  
37  
38  
39  
40  
41  
42  
43  
44  
45  
46  
47  
48  
49  
50  
51  
52  
53  
54  
55  
56  
57  
58  
59  
60

It is well known and the present study will corroborate that the behavior of FRP composites in longitudinal orientation ( $0^\circ$ ) is linear-elastic. It is well known that the optimum orientation of the fibers for enhancement of column strength under uniaxial compression is hoop direction. But in seismic design and strengthening, enhancement of column ductility using angle orientation can be desirable. Also in certain applications, such as eccentric compression loading, combination of axial load and bending moment, and slender columns, orienting the fibers of the FRP in the hoop direction may not offer the most enhancements of strength and ductility.

A number of studies have been conducted on various fiber orientations and wrap thicknesses in the civil engineering community. For example Mirmiran and Shahawy [3], Lam and Teng [7], Rochette and Labossiere [8], Pessiki et al. [9], Parvin and Jamwal [10, 11], Li et al. [12], Parvin and Wu [13], and Xiao and Wu [14] carried out many experiments on axially loaded concrete columns confined by FRP. These researchers have mainly concentrated on the behavior of concrete columns confined by FRP with various ply configurations. Some of these researchers have considered properties of FRP in complementary of their studies, but have not conducted a comprehensive study on tensile properties of FRP with various fiber orientations and their effects on confined concrete. For example Xiao and Wu [14] prepared three CFRP coupons with fiber oriented only at longitudinal orientation ( $0^\circ$ ) and carried out axial tension test for determination of ultimate stress, ultimate strain and elastic modulus.

In another study, Li et al. [12] prepared 15 GFRP coupons with three fiber orientations  $0^\circ$ ,  $45^\circ$  and  $90^\circ$  from the axial direction in one-ply and carried out axial tension test. In results, behavior of coupons with fibers oriented at  $45^\circ$  and  $90^\circ$  was classified such as pure resin without fibers. Lam and Teng [7] tested 35 CFRP coupons

1  
2  
3  
4 at longitudinal orientation in order to comparison with rupture stress and strain that  
5  
6 measured in tests on such FRP-confined concrete cylinders. They noted that  
7  
8 experimental stress-strain responses of the CFRP coupons were found to deviate slightly  
9  
10 from a perfectly linear relationship at the later stage of loading due to the gradual  
11  
12 stiffening of the CFRP as a result of the straightening of the fibers. In a different  
13  
14 approach, Yang et al [5] investigated degradation of strength and modulus of CFRP  
15  
16 laminates from fiber misalignment using tensile coupon tests. The specimens consisted  
17  
18 of one and two plies of unidirectional CFRP. The misalignment angles varied from 0 to  
19  
20 40° for the one-ply samples, and from 0 to 90° for the two-ply samples. It was  
21  
22 concluded that misalignment affects strength more than elastic modulus. However,  
23  
24 provided that mechanical parameters are related to the cross-sectional area of laminate  
25  
26 with fibers continuous from end to end of the coupon, the degradation of strength can be  
27  
28 accounted with a knock-down factor that is independent of misalignment angle.  
29  
30  
31  
32  
33  
34

35 On the other hand, and independently from the civil engineering community,  
36  
37 significant researches have taken place since the 1970s in the aerospace applications to  
38  
39 determine the source, and to assess the magnitude of, nonlinearity in the off-axis  
40  
41 direction in FRP structures [15]. For example, Hahn and Tsai [16], Hahn [17], and Hu  
42  
43 [18] reported that unidirectional FRP may exhibit severe nonlinearity in its in-plane  
44  
45 shear stress-strain relation. Haj-Ali and Kilic [19] carried out several tension,  
46  
47 compression, and shear tests on pultruded FRP coupons at different angles of 0°, 15°,  
48  
49 30°, 45°, 60°, and 90°. The overall linear elastic properties were identified along with the  
50  
51 nonlinear stress-strain behavior under the in-plane multi-axial tension and compression  
52  
53 loading.  
54  
55  
56  
57  
58  
59  
60

1  
2  
3  
4  
5  
6  
7  
8  
9  
10  
11  
12  
13  
14  
15  
16  
17  
18  
19  
20  
21  
22  
23  
24  
25  
26  
27  
28  
29  
30  
31  
32  
33  
34

Recently, Shao and Mirmiran [15] carried out an experimental investigation on coupons of two different types of laminated glass FRP tubes under tension and compression loading. First series tubes were made using centrifuge (spin) casting with 12.7 mm thickness and majority of the fibers in the longitudinal orientation. The wall thickness in these tubes consisted of a 7.6 mm structural laminate with symmetric lay-up of 40 plies in the form of  $[0^{\circ}/0^{\circ}/+45^{\circ}/-45^{\circ}]_{10}$  from E-glass and epoxy resin, a 4.6 mm resin-rich inner layer, and a 0.5 mm gel coating on the exterior. Second series tubes were filament wound with 5 mm thickness and  $\pm 55^{\circ}$  fiber orientation, also with E-glass and epoxy resin. However, these tubes did not have a resin layer or a gel coating. The two types of tubes represented two different failure modes; a brittle failure for W series with majority of the fibers in the longitudinal orientation, and a ductile failure for the thin tubes with off-axis fibers. The nonlinearity and ductility in these types of structures stem from the off-axis response of the FRP tube.

35  
36  
37  
38  
39

According to the previous researches on the subject, there are a number of issues that need to be addressed:

- 40  
41  
42  
43  
44  
45  
46  
47  
48
  - 49  
50  
51  
52  
53  
54  
55  
56  
57  
58  
59  
60
1. What are the effects of fiber orientation on stress-strain behavior, strength, stiffness, nonlinearity, and ductility of CFRP composites?
  2. What are the effects of nonlinear behavior of CFRP jackets on behavior of confined concrete columns?

The present study focuses on an investigation on tensile properties of CFRP composites in wrapped concrete columns. In response to the above questions, a number of CFRP coupons with different fiber orientations and various thicknesses were prepared and tested. Then an analytical modeling was performed on nonlinear behavior

of CFRP composites. The experimental and analytical studies are discussed in following sections.

## 2. Experimental Program

### 2.1. Specimens Layout

A total of 24 coupon specimens of CFRP composites with a width of about 30 mm and a length of 250 mm were prepared and tested under axial tension loading. The main experimental parameters include fiber orientation and number of plies. The test program and coupon properties are summarized in Table 1. Eight coupon series with different fiber orientations ( $0^\circ$ ,  $90^\circ$ ,  $0^\circ/90^\circ$ ,  $0^\circ/0^\circ$ ,  $0^\circ/0^\circ/0^\circ$ ,  $\pm 45^\circ$ ,  $+45^\circ/0^\circ/-45^\circ$ , and  $0^\circ/\pm 45^\circ/0^\circ$ ) were used; also all specimens were fabricated in triplicate. Figure 1 shows the typical geometry of coupon specimens. Gauge width, length, and thickness of every coupon were measured at three points and averages of them are summarized in Table 1. In this table L= longitudinal orientation of the fibers ( $0^\circ$ ); T= transverse orientation ( $90^\circ$ ); D= diagonal ( $+45^\circ$ ) and D'= diagonal ( $+135^\circ$  which is the same as  $-45^\circ$ ).

### 2.2. Material Properties and Specimens Preparation

A unidirectional carbon fiber sheet was used to prepare the CFRP coupons. Table 2 provides the properties of carbon fibers as supplied by the manufacturer. The carbon fiber sheet was cut with scissor and impregnated with epoxy resin by the hand lay-up technique. The epoxy resin consisted of two components, the main resin and the hardener. The mixing ratio of the components by weight was 100:15 and they were mixed for three minutes. The carbon fibers were configured in predefined orientations as shown in Table 1, and then were impregnated with the epoxy resin. Epoxy resin

1  
2  
3  
4 should be cured in laboratory temperature for a minimum of seven days. Table 3 shows  
5 the properties of cured resin as supplied by the manufacturer. Both ends of the coupons  
6 were tabbed by 30 mm wide and 50 mm long CFRP tabs attached by epoxy resin  
7 according to ASTM D3039/D3039M-95a standard [20] to avoid premature failure of the  
8 coupon ends.  
9  
10  
11  
12  
13  
14  
15  
16  
17

### 18 *2.3. Test Setup and Loading*

19  
20  
21 A hydraulic testing machine was used with hydraulic wedge grip assemblies in  
22 the Structure Laboratory of the Amirkabir University of Technology. Top grip assembly  
23 of the machine is vertical adjustable and it is attached to an actuator, while the bottom  
24 assembly is fixed. The coupons were first aligned with the centerline of the bottom grip.  
25 Each top and bottom grip-area of the coupon was 50 mm that were gripped. The coupons  
26 were tested in axial tension loading under displacement control mode with a rate of 0.5  
27 mm/min. The force and displacement data were obtained by data collecting system of  
28 the machine during the test and were filed by computer software.  
29  
30  
31  
32  
33  
34  
35  
36  
37  
38  
39  
40  
41  
42

## 43 **3. Experimental Results and Discussions**

44  
45 Experimental load-elongation curves of Specimens L, LL, and LLL are shown in  
46 Figure 2. The results reported are the average values for three identical specimens. The  
47 load-elongation curves show linear-elastic behavior up to the rupturing. With addition  
48 number of layers, stiffness and maximum load increase while maximum elongations do  
49 not change too much.  
50  
51  
52  
53  
54  
55

56  
57 Stress and strain in coupons were calculated with gauge thickness and gauge  
58 length of every coupon (see Table 1). The nominal thickness of carbon fiber sheet was  
59  
60



0.25 mm/ply, which was increased to 0.77 to 0.97 mm/ply when impregnated with epoxy resin. Figure 3 shows experimental stress-strain curve of Specimens L, T, and LT. The stress-strain curve of Specimens LL and LLL were close to Specimen L, the fiber orientation of these series is noted as longitudinal orientation. The tensile strength of CFRP composites in the longitudinal orientation was established to be approximately 303 MPa based on the fiber content corresponding to 0.92 mm/ply. This observation was found to be in agreement with the 3860 MPa fiber strength reported by the manufacturer (see Table 2). There is a difference between the maximum tensile strain of 1.6% specified by the manufacturer and the average ultimate strain of 0.74% recorded in the present tests. This difference is acceptable because a recent study by Ozbakkaloglu and Saatcioglu [21] has shown a similar result. The above mentioned values translate into an elastic modulus of 41 GPa for the composite material, which is in line with 242 GPa reported by the manufacturer for the modulus of elasticity of carbon fibers alone. Fiber orientations of Specimens T and LT are noted as matrix orientation and orthotropic orientation in sequence. The stress-strain curve of the matrix orientation shows linear-elastic behavior up to the rupturing and for the orthotropic orientation shows linear-elastic behavior up to the maximum strength and then softening behavior down to the ultimate strain. The longitudinal and matrix orientations have brittle rupture, but the orthotropic orientation has a brittle rupture with a little softening.

Figure 4 shows the stress-strain curve of Specimens L, DD', and LDD'L. The stress-strain of Specimens DD' and LDD'L show a nonlinear behavior that has basic different in comparison with the longitudinal, matrix, and orthotropic orientations. The fiber orientation of these series is noted as angle orientation. Stiffness and ultimate strength of the coupon with the angle orientation are less than the longitudinal

orientation, but strain ductility in the angle orientation is much more. The behavior of pure angle orientation (Specimen DD') is fully nonlinear, while the ultimate strain is 3.5%; equivalent yield strain by offset method is about 1%, for an offset strain of 0.2%. So strain ductility is calculated 3.5 for the pure angle orientation. The strain ductility ( $\mu$ ) as given by

$$\mu = \frac{\varepsilon_u}{\varepsilon_y} \quad (1)$$

where  $\varepsilon_u$  = ultimate strain; and  $\varepsilon_y$  = equivalent yield strain. For combination of longitudinal and angle orientations (Specimen LDD'L) the stress-strain curve shows a nonlinear behavior up to a maximum strength, and then down to a ductile failure with a nonlinear softening. This nonlinear behavior is very important for confined concrete with angle orientation (DD') that is discussed in the next section. Figure 5 shows the stress-strain curve of Specimens DD', DLD', and LDD'L. Comparison between the behaviors of Specimens DLD' and LDD'L shows that the softening behavior of the sticking together angle orientations (LDD'L) is better than the separated angle orientations (DLD'). Table 4 shows the average results of the CFRP coupon tests.

#### 4. Analytical Modeling

In FRP-confined concrete, the passive lateral confining pressure depends on the stiffness of the FRP jacket and increases continuously with the hoop strain of FRP [22]. So the stress-strain behavior of the FRP jacket in hoop direction of circular columns is very important. Some available confinement models for FRP-confined concrete such as those presented by Samaan et al. [23] and Teng et al. [22] were based on linear-elastic and non-yielding behavior of the FRP jacket, while off-axis orientation from hoop

direction can be used in many applications as well as mentioned in the first section. So there is a need to develop appropriate models for nonlinear behavior of the FRP jackets.

The nonlinear behavior of the angle orientation ( $\pm 45^\circ$ ) can be modeled by a parabolic curve as shown in Figure 6. A good correlation is noted with  $R^2 = 98.6\%$ . Based on the Figure 6, in general form, the stress-strain model of CFRP jacket in hoop direction is proposed by authors as follows:

$$f_f = \frac{E_{fi}^2}{4f_{fu}} \varepsilon_f \left( \frac{4f_{fu}}{E_{fi}} - \varepsilon_f \right) \quad (2)$$

where  $f_f$  and  $\varepsilon_f$  = stress and strain;  $E_{fi}$  = initial modulus; and  $f_{fu}$  = ultimate (maximum) strength of CFRP. This simple model is made with two parameters, the initial modulus and the ultimate strength of CFRP in the hoop direction that can be found easily. Tangent modulus ( $E_f$ ) can be derived by

$$E_f = \frac{\partial f_f}{\partial \varepsilon_f} = E_{fi} \left( 1 - \frac{E_{fi}}{2f_{fu}} \varepsilon_f \right) \quad (3)$$

The initial modulus is depended to the elastic modulus of CFRP in the longitudinal orientation and the orientation angle ( $\theta$ ) from the hoop direction. So it can be calculated by laminate theory principles as

$$\frac{1}{E_{fi}} = \frac{\cos^4 \theta}{E_1} + \left( \frac{1}{G_{12}} - \frac{2\nu_{12}}{E_1} \right) \sin^2 \theta \cdot \cos^2 \theta + \frac{\sin^4 \theta}{E_2} \quad (4)$$

where  $E_1$  and  $E_2$  = elastic modulus in the longitudinal and matrix orientation;  $G_{12}$  = major shear modulus; and  $\nu_{12}$  = major Poisson's ratio. The elastic modulus of  $E_1$  and  $E_2$  are obtained from the Table 4 equal to 41000 MPa and 2400 MPa in sequence. The major Poisson's ratio is assumed 0.25 and the major shear modulus of  $G_{12}$  is calculated by

$$\frac{1}{G_{12}} = \frac{1}{E_1} + \frac{1}{E_2} + \frac{2\nu_{12}}{E_2} \quad (5)$$

It is mentioned that the laminate theory principles govern only in linear elastic region and can not explain the nonlinear behavior. The ultimate strength depends on failure criterion. It can be found by Tsai-Hill failure criterion as

$$\frac{1}{f_{fu}^2} = \frac{\cos^4 \theta}{X^2} + \left( \frac{1}{S^2} - \frac{1}{X^2} \right) \sin^2 \theta \cdot \cos^2 \theta + \frac{\sin^4 \theta}{Y^2} \quad (6)$$

where  $X$  and  $Y$  are ultimate tensile strength in the longitudinal and matrix orientation; and  $S$  is ultimate shear strength (in plane). The ultimate tensile strength of  $X$  and  $Y$  are selected from the Table 4 equal to 303 MPa and 29 MPa in sequence. The ultimate shear strength of  $S$  is calculated with a back analysis in angle orientation ( $\pm 45^\circ$ ) equal to 40 MPa.

According to the above procedure, the initial modulus and the ultimate strength of CFRP in off-axis orientation are calculated. Table 5 shows these two parameters for different orientation angles. So the proposed parabolic model (Equation 2) can be used in modeling of CFRP-confined concrete. The proposed stress-strain model has been drawn in Figure 7 for different orientation angles.

It is mentioned, the nonlinear behavior of CFRP composites in off-axis orientation that reported in this paper, is based on the limited coupon tests. So this subject requires supplementary experimental studies in order to have a wide data base for proposing a comprehensive model.

As this study indicates, by orienting the fibers in off-axis directions, we can get a nonlinear stress-strain up to failure. This is a potential benefit that could be offered in making a "ductile" FRP. This could be of great value not only for retrofit of columns but also for strengthening of flexural members, by allowing the fibers to break

1  
2  
3  
4 sequentially and thus introducing a more ductile failure. The ductile behavior of FRP  
5  
6 composites could put forward some benefits in retrofit of walls and floors for blast  
7  
8 loading as well as columns and beams for seismic loading.  
9  
10

## 11 12 13 14 **5. Conclusion**

15  
16 In an attempt to explain effects of fiber orientation on mechanical properties of  
17  
18 CFRP composites under axial loading, this paper has presented and compared results of  
19  
20 axial tension testing on 24 CFRP coupons. Eight ply configurations were prepared with  
21  
22 fiber oriented at  $0^\circ$ ,  $\pm 45^\circ$  and  $90^\circ$  from the axial direction and with 1, 2, 3 or 4 plies.  
23  
24 Stress-strain behavior in longitudinal orientation ( $0^\circ$ ) and matrix orientation ( $90^\circ$ ) is  
25  
26 perfectly linear with brittle rupture, but in angle orientation ( $\pm 45^\circ$ ), shows a fully  
27  
28 nonlinear behavior with a large plastic deformation. At combinations of  $0^\circ$  and  $\pm 45^\circ$ , the  
29  
30 stress-strain curve shows a nonlinear behavior up to a maximum strength, and then  
31  
32 down to a ductile failure with a nonlinear softening. Based on the experimental behavior  
33  
34 in the angle orientation ( $\pm 45^\circ$ ), an analytical model proposed for the nonlinear stress-  
35  
36 strain behavior in off-axis orientation. The nonlinear behavior is a potential benefit that  
37  
38 could be offered in making a ductile FRP.  
39  
40  
41  
42  
43  
44  
45  
46  
47

## 48 **Acknowledgement**

49  
50 The authors acknowledge the financial assistances of the Amirkabir University  
51  
52 of Technology (Tehran Polytechnic) through, which enabled conducting this research.  
53  
54 The technical assistance of H. Motamedi, S. Afshar Rad and M.S. Khaleghi  
55  
56 Moghaddam of the Amirkabir University of Technology are appreciated.  
57  
58  
59  
60

## References

- [1] Sadeghian, P., Rahai, A. R. and Ehsani, M. R. (2007). Numerical Modeling of Concrete Cylinders Confined with CFRP Composites, *J Reinforced Plastic and Compos*, (in press).
- [2] Mander, J. B., Priestley, M. J. N. and Park, R. J. T. (1988). Theoretical Stress–Strain Model for Confined Concrete, *J Struct Engng ASCE*, 114(8): 1804–1826.
- [3] Mirmiran, A. and Shahawy, M. (1997). Behavior of Concrete Columns Confined by Fiber Composites, *J Struct Engng ASCE*, 123(5): 583–590.
- [4] Mirmiran, A. and Shahawy, M. (1997). Dilation Characteristics of Confined Concrete, *Int J Mech Cohesive-Frictional Materials*, 12(3): 237–249.
- [5] Yang, X., Nanni, A., Haug, S. and Sun, C. L. (2002). Strength and Modulus Degradation of Carbon Fiber-Reinforced Polymer Laminates from Fiber Misalignment, *J Mater Civil Engng ASCE*, 4(4): 320–326.
- [6] Mirmiran, A., Shahawy, M., Samaan, M., El Echary, H., Mastrapa, J. C. and Pico, O. (1998). Effect of Column Parameter on Fiber-Confined Concrete, *J Compos Construct ASCE*, 2(4): 175–185.
- [7] Lam, L. and Teng, J. G. (2004). Ultimate Condition of Fiber Reinforced Polymer-Confined Concrete, *J Compos Construct ASCE*, 8(6): 539–548.
- [8] Rochette, P. and Labossiere, P. (2000). Axial Testing of Rectangular Column Models Confined with Composites, *J Compos Construct ASCE*, 4(3): 129–136.
- [9] Pessiki, S., Harries, K., Kestner, J. T., Sause, R. and Ricles, J. M. (2001). Axial Behavior of Reinforced Concrete Columns Confined with FRP Jackets, *J Compos Construct ASCE*, 5(4): 237–245.

- 1  
2  
3  
4  
5 [10] Parvin, A. and Jamwal, A. S. (2005). Effects of Wrap Thickness and Ply  
6 Configuration on Composite-Confined Concrete Cylinders, *Compos Struct*, 67(4):  
7 437–442.  
8  
9  
10  
11 [11] Parvin, A. and Jamwal A. S. (2006). Performance of Externally FRP Reinforced  
12 Columns for Changes in Angle and Thickness of the Wrap and Concrete strength,  
13 *Compos Struct*, 73(4): 451–457.  
14  
15  
16 [12] Li, G., Maricherla, D., Singh, K., Pang, S. and John, M. (2006). Effect of Fiber  
17 Orientation on the Structural Behavior of FRP Wrapped Concrete Cylinders,  
18 *Compos Struct*, 74(4): 475–483.  
19  
20  
21 [13] Parvin, A. and Wu, S. (2007). Ply Angle Effect on Fiber Composite Wrapped  
22 Reinforced Concrete Beam-Column Connections under Combined Axial and  
23 Cyclic Loads, *Compos Struct*, (in press).  
24  
25  
26 [14] Xiao, Y. and Wu, H. (2000). Compressive Behavior of Concrete Confined by  
27 Carbon Fiber Composite Jackets, *J Mater Civil Engng ASCE*, 21(2): 139–146.  
28  
29  
30 [15] Shao, Y. and Mirmiran, A. (2004). Nonlinear Cyclic Response of Laminated Glass  
31 FRP Tubes Filled with Concrete, *Compos Struct*, 65(1): 91–101.  
32  
33  
34 [16] Hahn, T. and Tsai, S. (1973). Nonlinear Elastic Behavior of Unidirectional  
35 Composite Laminate, *J Compos Mater*, 7(1): 102–118.  
36  
37  
38 [17] Hahn, T. (1973). Nonlinear Behavior of Laminated Composites, *J Compos Mater*,  
39 7(4): 257–271.  
40  
41  
42 [18] Hu, H. (1993). Buckling Analyses of Fiber-Composite Laminate Shells with  
43 Material Non-linearity, *J Compos Technol Res*, 15(3): 202–208.  
44  
45  
46 [19] Haj-Ali, R. and Kilic, H. (2002). Nonlinear Behavior of Pultruded FRP  
47 Composites, *Compos Part B: Engng*, 33(1): 173–191.  
48  
49  
50  
51  
52  
53  
54  
55  
56  
57  
58  
59  
60

- 1  
2  
3  
4 [20] ASTM. (1995). *Standard Test Method for Tensile Properties of Polymer Matrix*  
5  
6 *Composite Material*, ASTM D3039/D3039M. West Conshohocken, Pa.  
7  
8  
9 [21] Ozbakkaloglu, T. and Saatcioglu, M. (2007). Seismic Performance of Square  
10  
11 High-Strength Concrete Columns in FRP Stay-in-Place Formwork, *J Struct Engng*  
12 *ASCE*, 133(1): 44–56.  
13  
14  
15 [22] Teng, J. G., Huang, Y. L., Lam, L. and Ye, L. P. (2007). Theoretical Model for  
16  
17 Fiber-Reinforced-Polymer-Confined Concrete, *J Compos Construct ASCE*, 1(2):  
18  
19 201–210.  
20  
21  
22 [23] Samaan, M., Mirmiran, A. and Shahawy, M. (1998). Model of Concrete Confined  
23  
24 by Fiber Composites, *J Struct Engng ASCE*, 124(9): 1025–1031.  
25  
26  
27  
28  
29  
30  
31  
32  
33  
34  
35  
36  
37  
38  
39  
40  
41  
42  
43  
44  
45  
46  
47  
48  
49  
50  
51  
52  
53  
54  
55  
56  
57  
58  
59  
60



Table 1. Test program and coupon properties

Coupon series	Coupon number	Number of plies	Fiber orientation	Gauge width (mm)	Gauge length (mm)	Gauge thickness (mm)	Thickness per ply (mm)
L	L-1	1	0°	29.0	150	0.92	0.92
	L-2			29.4	148	0.90	0.90
	L-3			29.1	150	0.92	0.92
T	T-1	1	90°	28.5	150	0.88	0.88
	T-2			29.2	152	0.88	0.88
	T-3			26.9	155	0.97	0.97
LT	LT-1	2	0°/90°	30.7	150	1.85	0.93
	LT-2			29.2	152	1.83	0.91
	LT-3			28.9	150	1.83	0.91
LL	LL-1	2	0°/0°	28.9	150	1.78	0.89
	LL-2			28.7	150	1.85	0.93
	LL-3			29.2	150	1.78	0.89
LLL	LLL-1	3	0°/0°/0°	29.7	150	2.70	0.90
	LLL-2			31.9	152	2.58	0.86
	LLL-3			29.7	153	2.64	0.88
DD'	DD'-1	2	±45°	29.6	146	1.58	0.79
	DD'-2			25.8	150	1.68	0.84
	DD'-3			30.0	152	1.60	0.80
DLD'	DLD'-1	3	+45°/0°/-45°	31.4	150	2.43	0.81
	DLD'-2			34.0	150	2.43	0.81
	DLD'-3			32.4	150	2.40	0.80
LDD'L	LDD'L-1	4	0°/±45°/0°	29.8	151	3.13	0.78
	LDD'L-2			30.4	152	3.20	0.80
	LDD'L-3			29.1	152	3.07	0.77

Table 2. Properties<sup>a</sup> of unidirectional carbon fibers

Fibers	Ultimate tensile strength (MPa)	Elastic modulus (GPa)	Ultimate strain (%)	Nominal thickness (mm/ply)	Areal weight (g/m <sup>2</sup> )
Carbon	3860	242	1.6	0.25	332

<sup>a</sup>Reported by the manufacturer.

For Peer Review

Table 3. Properties<sup>a</sup> of cured epoxy resin and hardener

Material	Tension		Compression		Shear
	Ultimate strength (MPa)	Elastic modulus (MPa)	Ultimate strength (MPa)	Elastic modulus (MPa)	Ultimate strength (MPa)
Epoxy	76.1	2789	97.4	937	54.8

<sup>a</sup> Reported by the manufacturer.

For Peer Review

Table 4. Average results of CFRP coupon tests

Fiber orientation	Ultimate strength (MPa)	Initial modulus (MPa)	Ultimate strain (%)	Strain ductility
Longitudinal orientation ( $0^\circ$ )	303	41000	0.74	1.0
Matrix orientation ( $90^\circ$ )	29	2400	0.72	1.0
Orthotropic orientation ( $0^\circ/90^\circ$ )	100	17000	0.97	1.6
Angle orientation ( $\pm 45^\circ$ )	47	3750	3.50	3.5
Angle orientation ( $0^\circ/\pm 45^\circ/0^\circ$ )	140	22000	3.20	3.7
Angle orientation ( $+45^\circ/0^\circ/-45^\circ$ )	117	17000	3.10	4.1

Table 5. Mechanical properties of CFRP composites in off-axis orientations

Orientation angle, $\theta$ (deg)	Ultimate strength, $f_{fu}$ (MPa)	Initial modulus, $E_{fi}$ (MPa)
0	303	41000
15	137	15892
30	72	6280
45	47	3710
60	36	2814
75	31	2484
90	29	2400

1  
2  
3  
4  
5  
6  
7 Figure 1. Typical geometry of coupon specimen  
8  
9

10 Figure 2. Experimental load-elongation curves of Specimens L, LL, and LLL  
11  
12

13 Figure 3. Experimental stress-strain curves of Specimen L, T, and LT  
14  
15  
16

17 Figure 4. Experimental stress-strain curves of Specimen L, DD', and LDD'L  
18  
19

20 Figure 5. Experimental stress-strain curves of Specimen DD', DLD', and LDD'L  
21  
22  
23

24 Figure 6. Modeling of nonlinear behavior in angle orientation ( $\pm 45^\circ$ )  
25  
26  
27

28 Figure 7. Proposed nonlinear stress-strain model for angle orientation ( $\pm\theta$ )  
29  
30  
31  
32  
33  
34  
35  
36  
37  
38  
39  
40  
41  
42  
43  
44  
45  
46  
47  
48  
49  
50  
51  
52  
53  
54  
55  
56  
57  
58  
59  
60

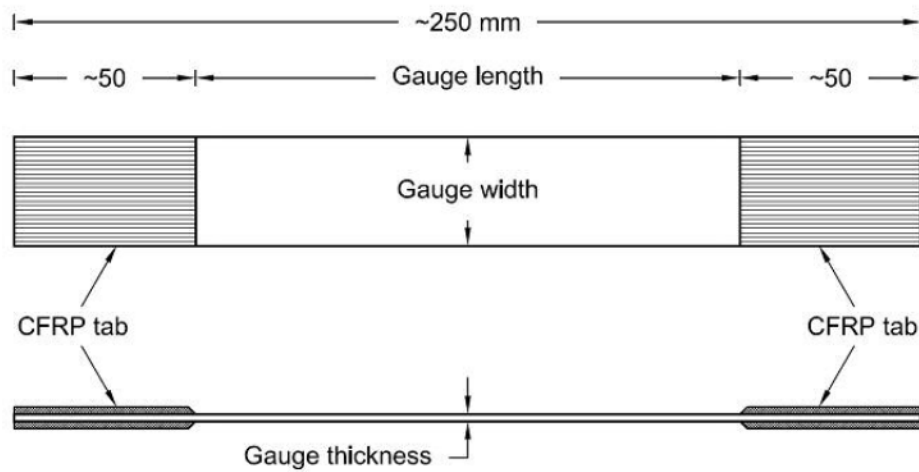


**Figure 1. Typical geometry of coupon specimen**  
193x104mm (96 x 96 DPI)

1  
2  
3  
4  
5  
6  
7  
8  
9  
10  
11  
12  
13  
14  
15  
16  
17  
18  
19  
20  
21  
22  
23  
24  
25  
26  
27  
28  
29  
30  
31  
32  
33  
34  
35  
36  
37  
38  
39  
40  
41  
42  
43  
44  
45  
46  
47  
48  
49  
50  
51  
52  
53  
54  
55  
56  
57  
58  
59  
60

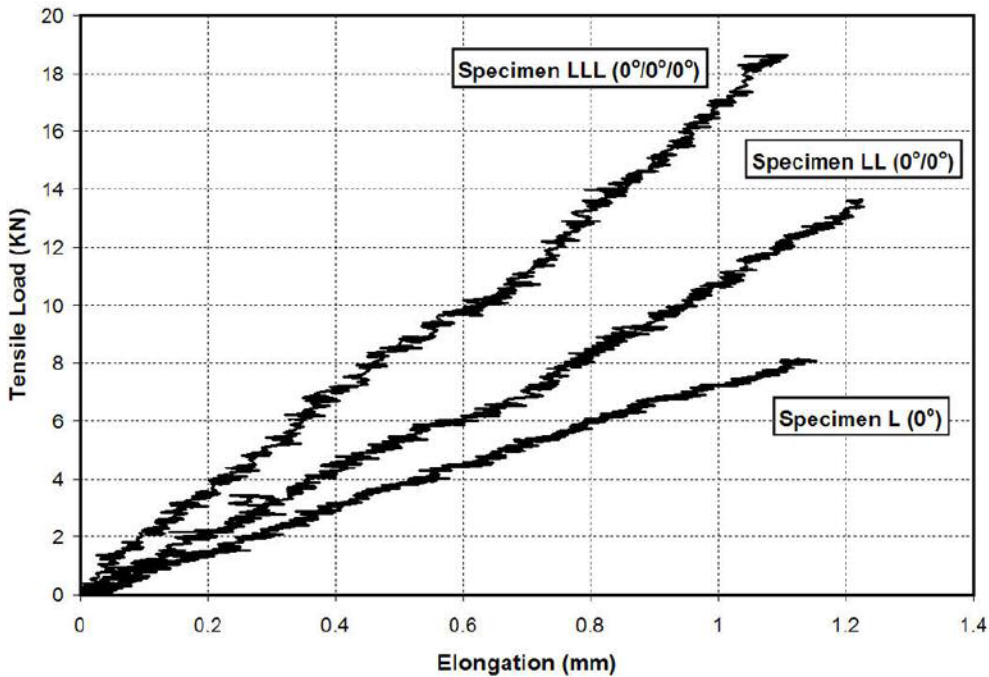


Figure 2. Experimental load-elongation curves of Specimens L, LL, and LLL  
222x153mm (96 x 96 DPI)



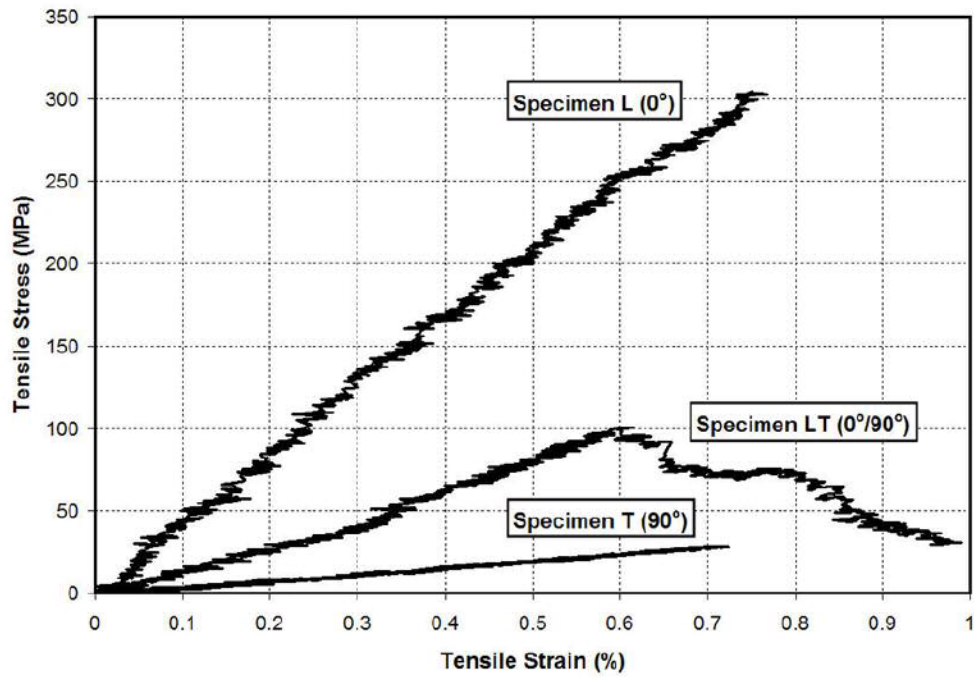


Figure 3. Experimental stress-strain curves of Specimen L, T, and LT  
224x155mm (96 x 96 DPI)

1  
2  
3  
4  
5  
6  
7  
8  
9  
10  
11  
12  
13  
14  
15  
16  
17  
18  
19  
20  
21  
22  
23  
24  
25  
26  
27  
28  
29  
30  
31  
32  
33  
34  
35  
36  
37  
38  
39  
40  
41  
42  
43  
44  
45  
46  
47  
48  
49  
50  
51  
52  
53  
54  
55  
56  
57  
58  
59  
60

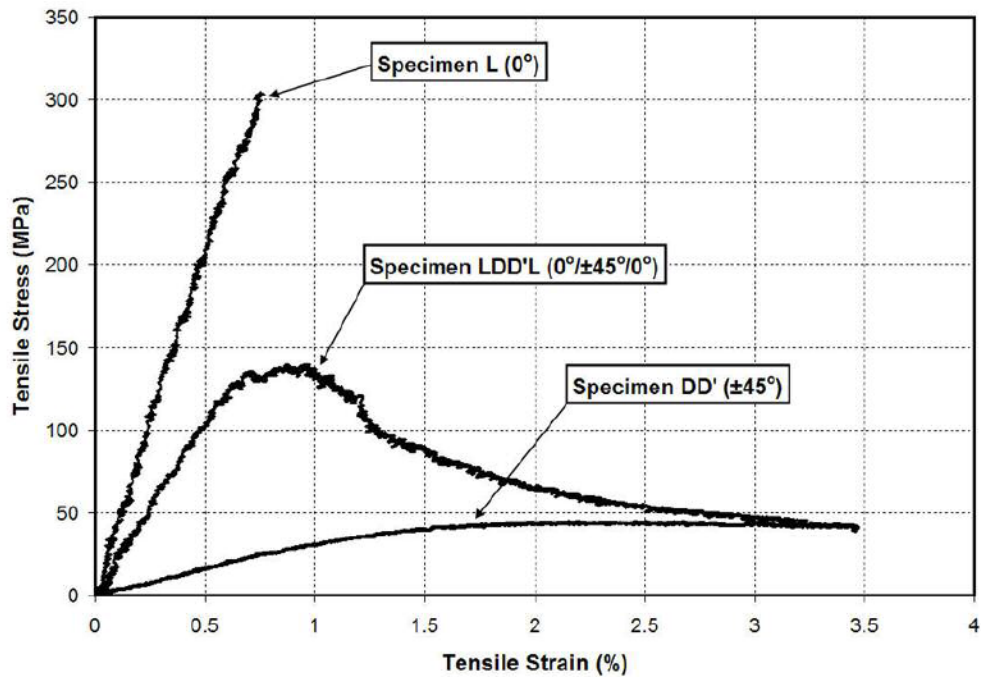


Figure 4. Experimental stress-strain curves of Specimen L, DD'□□, and LDD'□□L 224x155mm (96 x 96 DPI)

Review

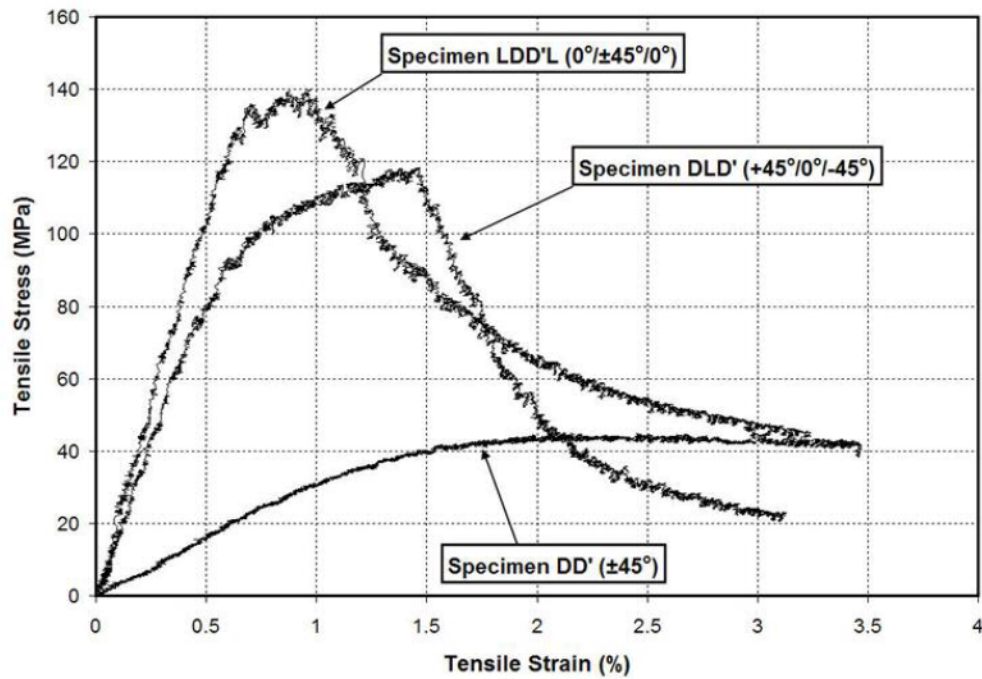
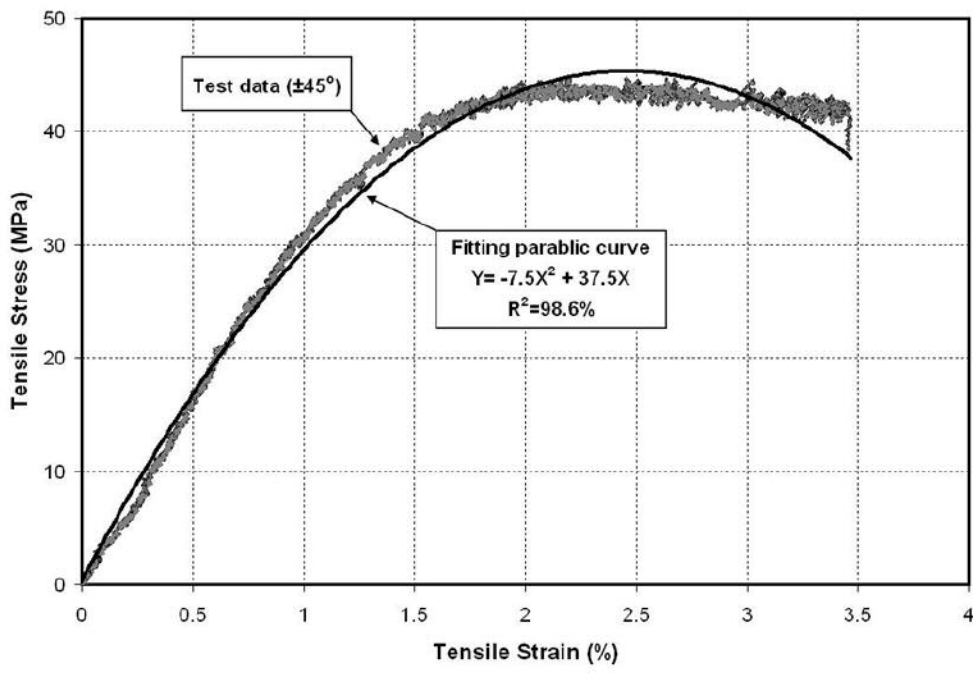


Figure 5. Experimental stress-strain curves of Specimen DD' (±45°), DLD' (+45°/0°/-45°), and LDD'L (0°/±45°/0°) 196x135mm (96 x 96 DPI)

1  
2  
3  
4  
5  
6  
7  
8  
9  
10  
11  
12  
13  
14  
15  
16  
17  
18  
19  
20  
21  
22  
23  
24  
25  
26  
27  
28  
29  
30  
31  
32  
33  
34  
35  
36  
37  
38  
39  
40  
41  
42  
43  
44  
45  
46  
47  
48  
49  
50  
51  
52  
53  
54  
55  
56  
57  
58  
59  
60



**Figure 6. Modeling of nonlinear behavior in angle orientation ( $\hat{A}\pm 45^\circ$ )**  
223x152mm (96 x 96 DPI)

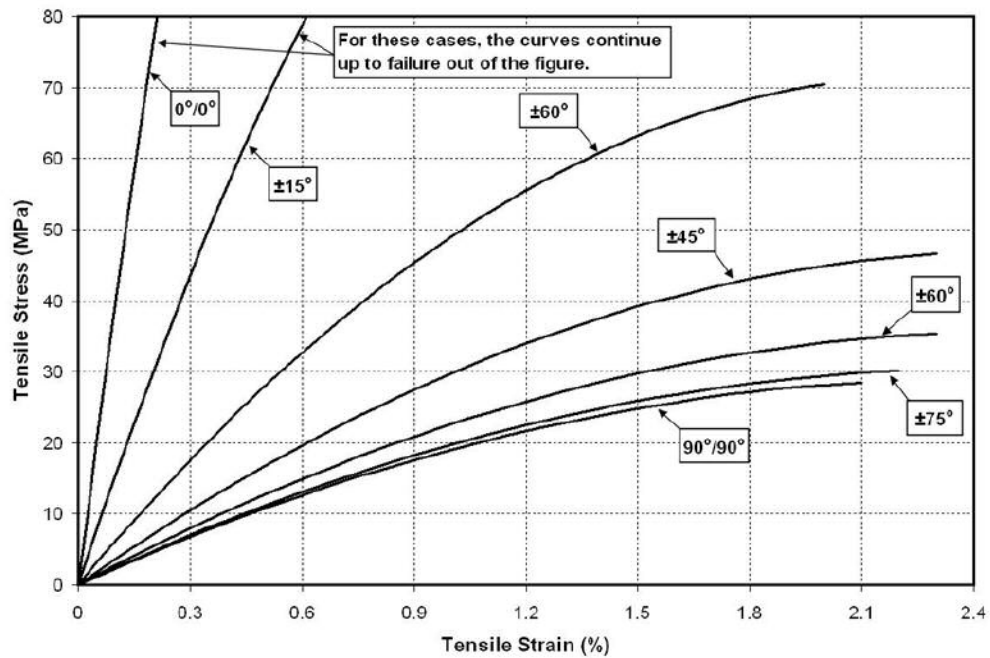


Figure 7. Proposed nonlinear stress-strain model for angle orientation ( $\hat{A}\pm\hat{I}$ , )  
221x149mm (96 x 96 DPI)